

## THERMAL DEGRADATION STUDIES ON SOME LANTHANIDE–EDTA COMPLEXES CONTAINING HYDRAZINIUM CATION

L. Vikram, B. Raju, R. Ragul and B. N. Sivasankar\*

Department of Chemistry, Government Arts College, Udhamandalam, The Nilgiris 643 002, India

Lighter and heavier lanthanide(III) ions react with dihydrazinium salts of ethylenediaminetetraacetic acid ( $H_4\text{edta}$ ) in aqueous solution to yield hydrazinium lanthanide ethylenediaminetetraacetate hydrate,  $N_2H_5[Ln(\text{edta})(H_2O)_3]\cdot(H_2O)_5$  where  $Ln=La, Ce, Pr, Nd, Sm, Eu, Gd, Tb$  and  $Dy$ . The numbers of water molecules present inside the coordination sphere have been confirmed by X-ray single crystal studies. The presence of five water molecules as lattice water is clearly shown by the mass loss from the TG analyses. Dehydration of a known amount (1 g) of each sample were carried out at constant temperature (100–110°C) for about 5 min further confirms the number of non-coordinated water molecules. The complexes after the removal of lattice water undergo multi-step decomposition to give respective metal oxide as the final product. The DTA shows endotherms for dehydration and exotherms for the decomposition of the anhydrous complexes. The formation of the metal oxides was confirmed by X-ray powder diffraction studies.

**Keywords:** coordinated water, edta complexes, hydrazinium cation, lanthanide oxides, lattice water, thermal degradation

### Introduction

Lanthanide ions aqueous solutions forms  $[Ln(H_2O)_n]^{3+}$ . Species from which substitution of water molecules by other ligands is generally difficult. However, ligands containing oxygen and nitrogen donor atoms are capable of coordination with lanthanide ions by replacing water molecules. These ligands form chelates which are usually more stable than the aquo complexes. Recently some lanthanide complexes, the preparation and thermal properties of rare earth elements complexes with 1,3,5-benzenetricarboxylic acid [1] and thermoanalytical and spectral properties of new rare-earth metal 2-pyrazinecarboxylate hydrates [2] have also been reported. Hence lanthanides are expected to form stable complexes with amino acids, polyaminocarboxylic acids and aromatic carboxylic acids.  $H_4\text{edta}$  is a polydentate ligand which coordinates with metal ions in different fashion. Though some lanthanide–edta complexes [3–6] and a few ammonium and potassium [7] salts of  $Ln$ –edta,  $[Ln(\text{edta})]$  are known, corresponding hydrazinium complexes have not been thoroughly investigated [8, 9]. Further, presence of hydrazinium ion in  $Ln$ –edta complexes greatly influences their thermal degradation behavior. Hydrazinium ion,  $N_2H_5^+$  with N–N bond which is endothermic nature, during thermal degradation results in the liberation of large quantity of heat energy by the cleavage of N–N bond [10]. Hence, the complexes containing  $N_2H_5^+$  group are expected to decompose at lower temperature than the corresponding simple  $Ln$ –edta complexes. The lone pair of electron present in one of the nitrogen atoms of  $N_2H_5^+$  ion is still capable of

coordination [11]. Hence, the nature of  $N_2H_5^+$  ions and its effect on the thermal degradation also gains much interest. In this paper we report the thermal degradation studies on some rare hydrazinium lanthanide ethylenediaminetetraacetate hydrates.

### Experimental

#### Materials and methods

The solvent were distilled prior to use and double distilled water was used for the preparation and analyses. The chemicals used were of AR grade received from SD Fine Chemicals. The hydrazine hydrate, 99–100% was used as such as received.

The complexes were prepared and characterized by the method reported earlier [8]. The simultaneous TG-DTA of the samples in static and dynamic air were recorded on a Netzsch STA 1500 simultaneous thermal analysis system, version V4.30, PL thermal sciences Division, UK in the temperature range 30–800°C using 2.5–5 mg of the samples with platinum cups as sample holders. The heating rate employed was  $10^\circ\text{C min}^{-1}$  the X-ray powder diffraction patterns of the residues were recorded using a Philips X-ray diffractometer model 1050/70 employing  $\text{CuK}_\alpha$  radiation of wavelength  $\lambda=1.5406 \text{ \AA}$  and recorded between 80 and  $10^\circ$ ,  $2\theta$  values at a scan rate of  $2^\circ \text{ min}^{-1}$ .

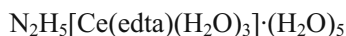
### Results and discussion

Hydrazinium ethylenediaminetetraacetatotriaquo-lanthanatepentaohydrate complexes,

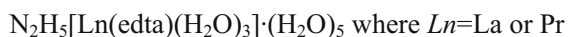
\* Author for correspondence: sivabickol@yahoo.com

$N_2H_5[Ln(edta)(H_2O)_3] \cdot (H_2O)_5$  have been prepared by the aqueous reaction between dihydraziniumdihydrogenethylenediamine-tetraacetate and the respective lanthanide(III) nitrate hydrates in 2:1 molar ratio. The crystalline complexes isolated from the aqueous solutions are stable, soluble in water and insoluble in organic solvents such as alcohol, ether and chloroform. These complexes undergo decomposition without melting as evidenced by TG-DTA studies, the composition and structure of the complexes were confirmed by chemical analyses, spectral and X-ray studies [8, 12].

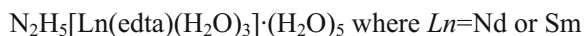
#### *Thermal degradation in static air*



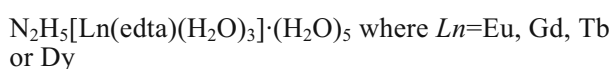
The first stage of degradation is dehydration resulting in the removal of five lattice water molecules and takes place between 50–95°C. The TG shows one step degradation corresponding to this dehydration. The mass loss observed is ~15% which is in accordance with the expected value. This stage is endothermic in DTA which shows a minimum at 75°C. The second stage of degradation takes place in the wide temperature range, between 90–255°C, which is assigned to the dehydratization. The proposed intermediate  $[Ce(Hedta)(H_2O)_3]$  further dehydrates continuously up to 375°C to give anhydrous  $[Ce(Hedta)]$ . This  $[Ce(Hedta)]$  decomposes in two stages, both exothermic with two sharp peaks in DTA observed at 420 and 455°C to give  $CeCO_3$  as the final residue below 550°C and  $Ce_2(C_2O_4)_3$  being the intermediate. The final mass loss observed in TG is 34% which is very close to the calculated value.



The first three stages are similar to that of the cerium complex. However, the La(Hedta) and Pr(Hedta) formed around 400°C were found to decompose gradually up to 520°C and above this temperature decompose sharply between 520–560°C to give respective oxalates which at higher temperature yield the respective carbonates below 750°C.



These complexes decompose almost similar to that of the praseodymium complex and the only difference observed is the TG temperature ranges for various stages and DTA peak temperatures.



These complexes show similar pattern of decomposition such as dehydration (of lattice water), dehydratization and ligand pyrolysis to give the respective lanthanide

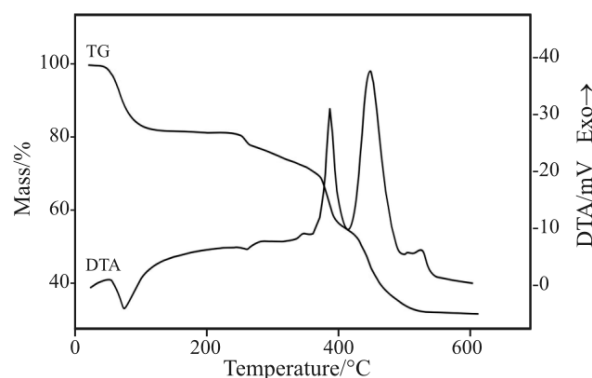


**Fig. 1** Simultaneous TG-DTA of  $N_2H_5[Ce(edta)(H_2O)_3](H_2O)_5$  in static air

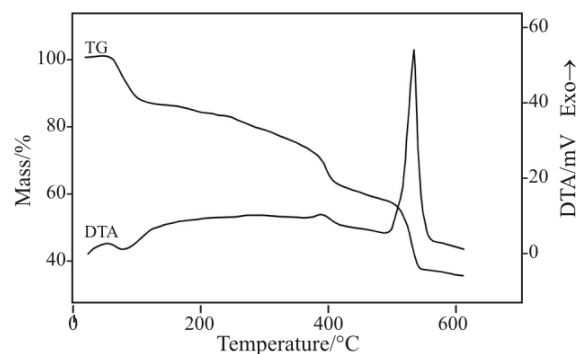


**Fig. 2** Simultaneous TG-DTA of  $N_2H_5[Sm(edta)(H_2O)_3](H_2O)_5$  in static air

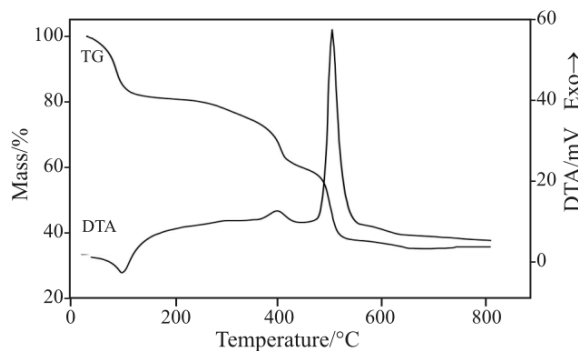


**Fig. 3** Simultaneous TG-DTA of  $N_2H_5[Gd(edta)(H_2O)_3](H_2O)_5$  in static air

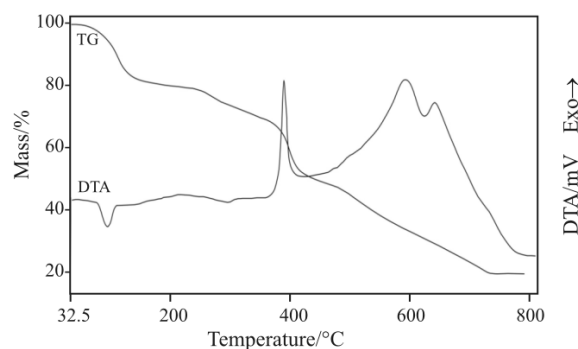


**Fig. 4** Simultaneous TG-DTA of  $N_2H_5[Dy(edta)(H_2O)_3](H_2O)_5$  in static air

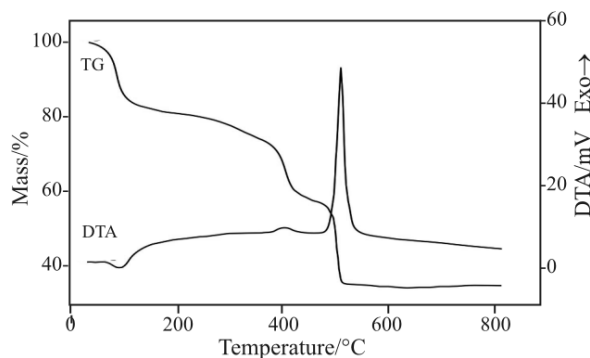
**Table 1** Data obtained from TG-DTA measurements in static air

Compound	Stage	TG temp. range/°C	DTA peak temp./°C	Mass loss/%		Final residue
				found	calc.	
$N_2H_5[La(edta)(H_2O)_3](H_2O)_5$ ( $LaC_{10}H_{33}O_{16}N_4$ )	I	50–100	80 (+)	14.00	14.91	A
	II	100–250	230 (–,w,b)	19.00	20.21	B
	III	250–350	290 (+,w)	30.00	29.15	C
	IV	350–420	410 (–,s)	56.00	55.16	D
	V	420–790	620 (–,s)	62.00	62.12	E
$N_2H_5[Ce(edta)(H_2O)_3](H_2O)_5$ ( $CeC_{10}H_{33}O_{16}N_4$ )	I	60–95	75 (+)	14.00	14.88	A
	II	90–260	250 (+,w,b)	21.00	20.17	B
	III	260–375	350 (–,w)	29.00	29.10	C
	IV	375–400	390 (–,s)	45.00	46.82	D*
	V	400–550	450 (–,s)	64.00	66.95	E*
$N_2H_5[Pr(edta)(H_2O)_3](H_2O)_5$ ( $PrC_{10}H_{33}O_{16}N_4$ )	I	50–90	75 (+)	13.00	14.86	A
	II	95–380	320 (–,w,b)	28.00	29.06	C
	III	380–405	390 (+,w)	52.00	54.98	D
	IV	405–650	550 (–,s)	63.00	61.912	E
$N_2H_5[Nd(edta)(H_2O)_3](H_2O)_5$ ( $NdC_{10}H_{33}O_{16}N_4$ )	I	51–100	75 (+)	13.00	14.78	A
	II	100–370	(w,b)	29.00	28.90	C
	III	370–405	380 (–,w)	53.00	54.68	D
	IV	405–720	545 (–,s)	61.00	61.57	E
$N_2H_5[Sm(edta)(H_2O)_3](H_2O)_5$ ( $SmC_{10}H_{33}O_{16}N_4$ )	I	55–105	80 (+,w)	13.00	14.63	A
	II	105–375	(w,b)	30.00	28.61	C
	III	375–410	385 (–,w)	45.50	46.46	D*
	IV	410–600	530 (–,s)	63.00	60.96	E
$N_2H_5[Eu(edta)(H_2O)_3](H_2O)_5$ ( $EuC_{10}H_{33}O_{16}N_4$ )	I	60–100	80 (+)	14.00	14.59	A
	II	100–240	220 (–,w,b)	20.00	19.78	B
	III	240–380	340 (+,w,b)	27.50	28.54	C
	IV	380–420	400 (–,s)	52.00	54.00	D
$N_2H_5[Gd(edta)(H_2O)_3](H_2O)_5$ ( $GdC_{10}H_{33}O_{16}N_4$ )	I	60–100	95 (+)	14.00	14.47	A
	II	100–250	220 (–,w,b)	20.00	19.61	B
	III	250–370	300 (+,w,b)	27.50	28.29	C
	IV	370–450	400 (–,s)	52.00	54.00	D
	V	450–530	505 (–,s)	62.00	60.80	E
$N_2H_5[Tb(edta)(H_2O)_3](H_2O)_5$ ( $TbC_{10}H_{33}O_{16}N_4$ )	I	60–120	100 (+)	15.00	14.43	A
	II	120–220	180 (–,w,b)	20.00	19.56	B
	III	220–350	320 (+,w,b)	30.00	28.22	C
	IV	350–430	410 (–,s)	52.00	53.40	D
	V	430–530	510 (–,s)	58.50	60.13	E
$N_2H_5[Dy(edta)(H_2O)_3](H_2O)_5$ ( $DyC_{10}H_{33}O_{16}N_4$ )	I	50–110	95 (+)	16.00	14.35	A
	II	110–240	220 (–,w,b)	20.00	19.45	B
	III	240–370	300 (+,w,b)	28.50	28.06	C
	IV	370–420	400 (–,s)	46.00	46.16	D*
	V	420–510	505 (–,s)	63.00	59.78	E

A:  $N_2H_5[Ln(edta)(H_2O)_3]$ , B:  $[Ln(Hedta)(H_2O)_3]$ , C:  $[Ln(Hedta)]$ , D:  $0.5Ln_2(C_2O_4)_3$ , D\*:  $[Ln(Hedta)_{0.75}]$ , E:  $0.5Ln_2(CO_3)_3$  and E\*:  $CeCO_3$ , +: endotherm, –: exotherm, b: broad, w: weak, s: sharp

carbonates as the final residue. It is surprising to note that even the TG temperature ranges and the DTA peak temperatures are very close and the mass losses for the respective stages are also very similar. Hence the TG–DTA traces are almost superimposable.

The data obtained from TG–DTA experiments of these complexes are summarized in Table 1 and the simultaneous TG–DTA traces of cerium, samarium, gadolinium and dysprosium complexes are shown in Figs 1–4 as representative examples.


**Fig. 5** Simultaneous TG-DTA of  $N_2H_5[Nd(edta)(H_2O)_3](H_2O)_5$

**Table 2** TG-DTA data in dynamic air

Compound	Stage	TG temp. range/°C	DTA peak temp./°C	Mass loss(%)		Final residue
				found	calc.	
N <sub>2</sub> H <sub>5</sub> [La(edta)(H <sub>2</sub> O) <sub>3</sub> ](H <sub>2</sub> O) <sub>5</sub> (LaC <sub>10</sub> H <sub>33</sub> O <sub>16</sub> N <sub>4</sub> )	I	50–200	90, 150 (+,d)	19.00	20.21	A
	II	200–400	290,350	30.00	29.15	C
	III	400–800	(w,b) (-,b,d)	71.50	73.04	F
N <sub>2</sub> H <sub>5</sub> [Ce(edta)(H <sub>2</sub> O) <sub>3</sub> ](H <sub>2</sub> O) <sub>5</sub> (CeC <sub>10</sub> H <sub>33</sub> O <sub>16</sub> N <sub>4</sub> )	I	50–80	70 (+)	15.00	14.88	A
	II	80–220	190 (-,w,b)	20.00	20.17	B
	III	220–360	320 (+,w)	30.00	29.10	C
	IV	360–420	390 (-,s)	48.00	46.82	D*
	V	420–530	510 (-,b)	69.00	71.57	F
N <sub>2</sub> H <sub>5</sub> [Pr(edta)(H <sub>2</sub> O) <sub>3</sub> ](H <sub>2</sub> O) <sub>5</sub> (PrC <sub>10</sub> H <sub>33</sub> O <sub>16</sub> N <sub>4</sub> )	I	50–130	100 (+)	14.00	14.86	A
	II	130–260	2000 (-,w,b)	20.00	20.14	B
	III	260–360	320 (+,w)	27.00	29.06	C
	IV	360–490	390 (-,s)	45.00	46.79	D*
	V	490–650	550 (-,b)	70.00	72.80	F
N <sub>2</sub> H <sub>5</sub> [Nd(edta)(H <sub>2</sub> O) <sub>3</sub> ](H <sub>2</sub> O) <sub>5</sub> (NdC <sub>10</sub> H <sub>33</sub> O <sub>16</sub> N <sub>4</sub> )	I	50–130	90 (+)	15.00	14.78	A
	II	130–300	250 (-,w,b)	20.00	20.03	B
	III	300–350	335 (+,w)	27.00	28.90	C
	IV	350–500	390 (-,s)	44.00	46.67	D*
	V	500–720	610,660 (-,b,d)	70.00	72.40	F
N <sub>2</sub> H <sub>5</sub> [Sm(edta)(H <sub>2</sub> O) <sub>3</sub> ](H <sub>2</sub> O) <sub>5</sub> (SmC <sub>10</sub> H <sub>33</sub> O <sub>16</sub> N <sub>4</sub> )	I	50–120	90 (+)	14.00	14.63	A
	II	120–275	210 (-,w,b)	19.00	19.83	B
	III	275–380	290 (+,w)	29.00	28.61	C
	IV	380–430	385 (-,s)	44.00	46.46	D*
	V	430–730	590,640 (-,b,d)	71.00	71.68	F
N <sub>2</sub> H <sub>5</sub> [Eu(edta)(H <sub>2</sub> O) <sub>3</sub> ](H <sub>2</sub> O) <sub>5</sub> (EuC <sub>10</sub> H <sub>33</sub> O <sub>16</sub> N <sub>4</sub> )	I	50–100	80 (+)	16.00	14.59	A
	II	100–270	(-,w,b)	21.00	19.78	B
	III	270–400	380 (+,w,b)	30.00	28.54	C
	IV	400–520	450 (-,s)	48.00	46.40	D*
	V	520–750	660,720 (-,s,d)	73.50	71.50	F
N <sub>2</sub> H <sub>5</sub> [Gd(edta)(H <sub>2</sub> O) <sub>3</sub> ](H <sub>2</sub> O) <sub>5</sub> (GdC <sub>10</sub> H <sub>33</sub> O <sub>16</sub> N <sub>4</sub> )	I	50–100	90 (+)	14.00	14.47	A
	II	100–240	(-,w,b)	18.50	19.61	B
	III	240–350	290 (+,w,b)	27.00	28.29	C
	IV	350–470	420 (-,s)	45.00	46.22	D*
	V	470–540	510 (-,s)	68.90	70.89	F
N <sub>2</sub> H <sub>5</sub> [Tb(edta)(H <sub>2</sub> O) <sub>3</sub> ](H <sub>2</sub> O) <sub>5</sub> (TbC <sub>10</sub> H <sub>33</sub> O <sub>16</sub> N <sub>4</sub> )	I	70–110	100 (+)	13.50	14.43	A
	II	110–260	(-,w,b)	18.50	19.56	B
	III	260–320	290 (+,w,b)	27.70	28.22	C
	IV	320–450	410 (-,s)	44.90	46.16	D*
	V	450–550	520 (-,s)	68.80	70.70	F
N <sub>2</sub> H <sub>5</sub> [Dy(edta)(H <sub>2</sub> O) <sub>3</sub> ](H <sub>2</sub> O) <sub>5</sub> (DyC <sub>10</sub> H <sub>33</sub> O <sub>16</sub> N <sub>4</sub> )	I	60–100	90 (+)	14.00	14.35	A
	II	100–250	(-,w,b)	18.50	19.45	B
	III	250–330	300 (+,w,b)	27.00	28.06	C
	IV	330–460	430 (-,s)	45.00	46.04	D*
	V	460–550	530 (-,s)	69.00	70.30	F

A: N<sub>2</sub>H<sub>5</sub>[Ln(edta)(H<sub>2</sub>O)<sub>3</sub>], B: [Ln(Hedta)(H<sub>2</sub>O)<sub>3</sub>], C: [Ln(Hedta)], D: 0.5Ln<sub>2</sub>(C<sub>2</sub>O<sub>4</sub>)<sub>3</sub>, D\*: [Ln(Hedta)<sub>0.75</sub>], F: Ln<sub>2</sub>O<sub>3</sub>, +: endotherm, -: exotherm, b: broad, w: weak, s: sharp and d: doublet

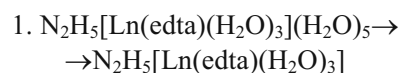
### Thermal degradation in dynamic air

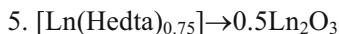
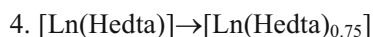
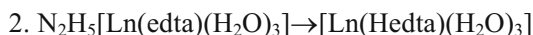
The present series of complexes have also been subjected to the thermal degradation in dynamic air. The results are different from those observed with static air.

The TG and DTA profiles for the complexes are similar to those observed static air till the formation of Ln(Hedta) intermediate. These intermediates in dynamic air undergo slow, gradual and continuous decomposition

in the wide temperature range, between 450–800°C to give invariably the respective oxides as the final residue. For each and every stage the temperature range is found to be higher than that observed with static air.

The probable scheme of degradation of the complexes in dynamic air is given below.





where  $\text{Ln} = \text{La}, \text{Ce}, \text{Pr}, \text{Nd}, \text{Sm}, \text{Eu}, \text{Gd}, \text{Tb}$  and  $\text{Dy}$ .

Hence in dynamic air the gaseous products such as  $\text{CO}, \text{CO}_2, \text{H}_2\text{O}, \text{N}_2$  etc., evolved during the degradation of the complexes are swept away and excludes the formation of respective stable lanthanide carbonates. In static air after the formation of  $\text{Ln}(\text{Hedta})$  the change in the trend of the TG curve is observed during the decomposition and it is not continuous indicating the formation of respective lanthanide oxalates which in the presence of evolved gases, especially in the presence of  $\text{CO}_2$  resulted in the formation of respective carbonates as the residue. However in dynamic air the formed  $\text{Ln}(\text{Hedta})$  undergo gradual decomposition and there is no sign in the thermal pattern for the formation of any other intermediate and the evolved gases are also removed and hence the respective lanthanide oxide formation is favored.

The TG-DTA data of the complexes in dynamic air is summarized in Table 2. The simultaneous TG-DTA profiles of neodymium and samarium

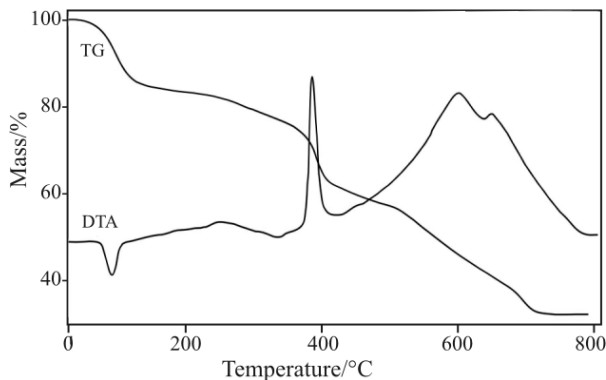


**Fig. 6** Simultaneous TG-DTA of  $\text{N}_2\text{H}_5[\text{Sm}(\text{edta})(\text{H}_2\text{O})_3](\text{H}_2\text{O})_5$  in dynamic air

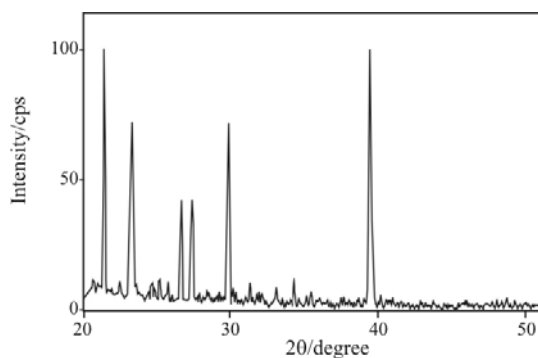


**Fig. 7** X-ray powder diffraction pattern of  $\text{Nd}_2\text{CO}_3$

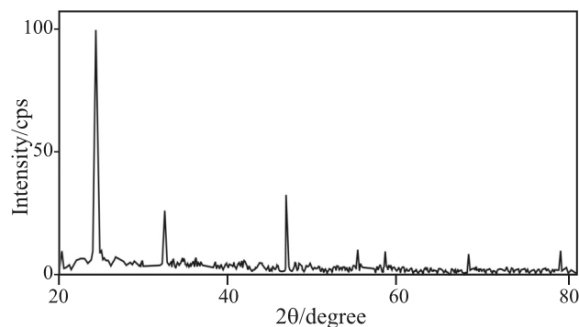


**Fig. 8** X-ray powder diffraction pattern of  $\text{Sm}_2\text{O}_3$

complexes are shown in Figs 5 and 6 respectively as representative examples.

Due to the continuous degradation we were not able to isolate the probable intermediates for further studies. They are proposed on the basis of TG mass loss. However the final residues were analyzed by chemical analysis and X-ray powder pattern. The X-ray powder pattern of the  $\text{Nd}_2(\text{CO}_3)_3$  and  $\text{Sm}_2\text{O}_3$  obtained as residues during the thermal degradation of the samarium complex in static and dynamic air respectively are shown in Figs 7 and 8, respectively.

## References

1. Z. Rzaczyńska, A. Ostasz and S. Pikus, *J. Therm. Anal. Cal.*, 82 (2005) 347.
2. S. Govindarajan, *J. Therm. Anal. Cal.*, 79 (2005) 685.
3. M. D. Lind, B. Lee and J. L. Hoard, *J. Am. Chem. Soc.*, 87 (1965) 1611.
4. L. Helmholz, *J. Am. Chem. Soc.*, 61 (1939) 1544.
5. J. L. Hoard, B. Lee and M. D. Lind, *J. Am. Chem. Soc.*, 87 (1965) 1612.
6. G. Anderegg, *Adv. Mol. Relax. Interact. Proc.*, 18 (1980) 79.
7. G. Wilkinson, R. D. Gillard and J. A. Mc Claverty, *Comprehensive Coordination Chemistry, The Synthesis, Reactions, Properties and Applications, Vol. 2, 1<sup>st</sup> Edn.*, Pergamon Press, London 1987.
8. L. Vikram and B. N. Sivasankar, *Indian J. Chem.*, 45A (2006) 864.
9. N. Saravanan, B. N. Sivasankar, S. Govindarajan and K. K. Mohammed Yusuff, *Synth. React. Inorg. Met.-Org. Chem.*, 24 (1994) 703.
10. A. Braibanti, F. Dallavalle, M. A. Pellinghelli and E. Leporati, *Inorg. Chem.*, 7 (1986) 1430.
11. E. W. Schmidt, 'Hydrazine and its Derivatives', John Wiley & Sons, Inc., 1984.
12. L. Vikram and B. N. Sivasankar, *Indian J. Chem.*, 47A (2008) 25.

Received: August 13, 2007

Accepted: January 22, 2008

OnlineFirst: June 26, 2008

DOI: 10.1007/s10973-007-8685-4